VERTICAL MOTIONS IN THE UPPER ATMOSPHERE DEDUCED FROM ROCKET MEASURED TEMPERATURES

By

C. Prabhakara

Goddard Space Flight Center
Institute for Space Studies
National Aeronautics and Space Administration

and

Joseph S. Hogan

Department of Meteorology and Oceanography
New York University

12/67

A B S T R A C T

Rocket observations at high latitudes indicate a significantly cold thermal structure during summer in the upper mesosphere and lower thermosphere. From detailed considerations of radiative transfer we have obtained the infrared heating rates in this region of the atmosphere and deduced vertical velocities from these heating rates.

We find that strong infrared flux convergence in the vicinity of 85 km results in a heating of about 10^{o} K/day and positive vertical velocities of about 5 cm/sec. Such vertical velocities favor the formation of noctilucent clouds at this altitude.

CONTENTS

	Page
Abstract.	i
Introduction.	1
Theoretical Considerations.	3
Transmission Functions.	7
Results and Discussion.	12
Acknowledgements.	15
References.	16

Vertical Motions in the Upper Atmosphere Deduced from Rocket Measured Temperatures

Introduction

Recent high-altitude rocket-grenade experiments at Churchhill, Canada, Barrow, Alaska and Kronogard, Sweden have revealed some interesting features of the temperature structure in the earth's mesophere and lower thermosphere. These observations indicate that, at high latitudes, this region of the atmosphere is significantly warmer in winter than in summer, as shown in Figure I (Theon, Nordberg and Smith, 1966). Such a temperature pattern cannot be explained by considering a radiation balance alone. It has been suggested that, in winter, dynamical heating (Leovy, 1964), chemical heating (Kellogg, 1961) and heating by dissipating gravity waves (Hines, 1963; Leovy, 1966) may play a role in establishing the thermal structure at these levels. In summer, however, dynamical cooling appears to be the only significant non-radiative process involved.

An examination of radiative heating and cooling in the stratosphere and mesosphere has been made by Murgatroyd and Goody (1958) using the information regarding the thermal structure of the atmosphere available at that time. On the basis of their heating rates, Murgatroyd and Singleton (1961) derived a meridional circulation in this region of the atmosphere.

The extremely cold temperature structure in the vicinity of the mesopause in summer, which has been revealed by the recent observations prompts us to re-examine the radiative balance of this region.

For the observed summer temperature structure at Kronogard and Barrow (Figures II and III) the infrared heating of the atmosphere at these levels is obtained from a detailed radiative transfer calculation in the 15 μ CO_2 and 9.6 μ O_3 bands. From this heating we derive the vertical velocities necessary to maintain the observed temperature structure, assuming solar ultraviolet heating is absent. Such estimates of vertical velocities are conservative, in our view, since any solar heating would only enhance vertical motions.

Theoretical Considerations

From the theory of radiative transfer, it is possible to calculate an equilibrium temperature structure when the sources and sinks of radiative energy within the atmosphere are known. Conversely, if a thermal structure is specified, for example, from observations, and if an assumption of quasi-equilibrium is made, the radiative heating and cooling rates in the atmosphere can be obtained.

The basic equation of radiative transfer relates the net flux divergence to the absorbed and emitted energies per unit volume and per unit time:

$$\iint \frac{dI(\nu,\theta,z)}{ds}\, d\nu\, d\omega = -\iint I(\nu,\theta,z)n(z)k(\nu,z)d\nu\, d\omega + \iint J(\nu,z)n(z)k(\nu,z)\, d\nu\, d\omega \qquad (1)$$

where the symbols have the following meaning:

ν	frequency of radiation
ω	solid angle
θ	zenith angle
s	geometric path length ($ds = \sec\theta\, dz$)
z	altitude
$n(z)$	number density of absorbing molecules
$k(\nu,z)$	absorption coefficient
$J(\nu,z)$	source function
$I(\nu,\theta,z)$	intensity of radiation .

With the boundary conditions of zero downward flux of infrared energy at the top of the atmosphere z_H, and a black-body surface at the ground z_o, the basic equation of radiative transfer (1) can be solved to yield at any level z_1, the upward and downward intensities, $I\uparrow(\nu,\theta, z_1)$ and $I\downarrow(\nu,\theta,z_1)$ respectively:

$$I\uparrow(\nu,\theta,z_1) = B(\nu,z_o)\tau(\nu,\theta,z_1 - z_o) + \int_{z_o}^{z_1} J(\nu,z)\frac{\partial\tau(\nu,\theta,z_1 - z)}{\partial z}dz \quad (2)$$

$$I\downarrow(\nu,\theta,z_1) = \int_{z_1}^{z_H} J(\nu,z)\ \frac{\partial\tau(\nu,\theta,z - z_1)}{\partial z}dz\ . \quad (3)$$

$B(\nu,z_o)$ is the Planck intensity from the ground, and $\tau(\nu,\theta,|z_1 - z|)$ represents the transmission of the atmosphere at frequency ν and zenith angle θ between levels z and z_1:

$$\tau(\nu,\theta,|z_1 - z|) = 1 - A(\nu,\theta,|z_1 - z|) \quad (4)$$

where $A(\nu,\theta,|z_1 - z|)$ is the fractional absorption.

From expressions (1), (2) and (3) the intensities and thereby the net flux divergence can be evaluated, provided the transmission function τ and the source function J are known. A discussion of the transmission function is given in the next section.

The source function J is commonly assumed to be the Plank intensity B. However, such an assumption fails in the 15 μ CO_2 band at low pressures in the high atmosphere, where molecular

collisions are not frequent enough to maintain the vibrational energy levels in a Boltzmann distribution. According to Curtis and Goody (1956) the source function in this band when there is departure from local thermodynamic equilibrium is given by:

$$J(\nu,z) = B(\nu,z)\left(1 - \frac{\lambda}{\varphi}\frac{\iint \frac{dI(\nu,\theta,z)}{ds}\, d\nu d\omega}{\iint B(\nu,z)n(z)k(\nu,z)\, d\nu d\omega}\right) \tag{5}$$

where φ is the radiative lifetime and λ is the vibrational relaxation lifetime.

Since the source function J shown in equation (5) is itself dependent on the flux divergence, $\iint \frac{dI(\nu,\theta,z)}{ds}\, d\nu d\omega$, in the 15 μ band, an iterative procedure is adopted to determine J.

Radiative transfer in the 9.6 μ O_3 band should be treated in a similar manner to allow for possible departure from thermodynamic equilibrium. A lack of knowledge of the relaxation time for the O_3 molecule prevents us from doing so, and we have assumed the validity of Kirchhoff's law in the 9.6 μ band. At high altitudes the flux divergence of energy in the 9.6 μ band is small compared to that in 15 μ CO_2 band, so that such an assumption does not lead to significant error.

Taking the temperature structure in the atmosphere from rocket observations we have computed the total infrared flux divergence in the 15 μ CO_2 band and 9.6 μ O_3 bands. Under steady state conditions, this total flux divergence must be balanced by solar energy absorption and dynamical heating, so that

$$-W(z)\rho(z)C_p\left(\frac{\partial T(z)}{\partial z}+\frac{g}{C_p}\right)+Q(z)=\iint\frac{dI(\nu,\theta,z)}{ds}\,d\nu d\omega \qquad (6)$$

where $W(z)$ is vertical velocity

$\rho(z)$ is mass density

C_p is specific heat at constant pressure

g is the acceleration due to gravity

$Q(z)$ is the solar energy absorbed per unit volume and per unit time by O_2 and O_3.

Equation (6) can be solved for $W(z)$ provided the other quantities involved are specified.

The solar ultraviolet energy absorbed by O_2 and O_3 can be evaluated by specifying the absorption cross sections, spectral energy distribution, and the local concentrations of O_2 and O_3. The vertical distribution of these gases may be obtained from photochemical considerations (See, for example, Prabhakara and Hogan, 1965).

Transmission Functions

The relative importance of Lorentz and Doppler broadening depends upon the region of the atmosphere under consideration. In the optically thick layers of the lower atmosphere, where collisions are frequent, line broadening is predominantly Lorentz in character. At very high levels, on the other hand, the Doppler broadening is important, while at intermediate heights, a combination of both Lorentz and Doppler effects is present. A general expression for the variation of the absorption coefficient over a spectral line which takes both phenomena into account is given by

$$k(\nu) = S \int_{-\infty}^{+\infty} \left(\frac{\nu_o}{\sqrt{\pi} c \alpha_D} \right) \exp - \left(\frac{\nu_o U}{c \alpha_D} \right)^2 \frac{\alpha_L}{\pi} \frac{dU}{(\nu - \nu_o + U\nu_o/c)^2 + \alpha_L^2} \quad (7)$$

Here, the symbols have the meaning:

S	total line intensity
U	molecular velocity
ν_o	central frequency of line
c	speed of light
α_L	Lorentz half-width of line
α_D	Doppler half-width of line.

For small values of the parameter $\alpha = \alpha_L/\alpha_D$, Harris (1948) has expressed this integral as a power series in α, with coefficients H_i which are tabulated as functions of the parameter $v = (\nu - \nu_o)/\alpha_D$:

$$k_v = \frac{S}{\sqrt{\pi}\alpha_D}[H_o(v) + \alpha H_1(v) + \alpha^2 H_2(v) + \ldots] \tag{8}$$

This formulation was used to evaluate k_v for $\alpha < 0.5$. Using this expression, the mean fractional absorption for a spectral interval is

$$A = \frac{\alpha_D}{d}\int_{-d/2\alpha_D}^{+d/2\alpha_D}[1 - \exp(-k_v u)]dv \tag{9}$$

where d is the mean line spacing and u is the optical path. Equation (9) can be solved numerically by substituting the tabulated functions H_i in equation (8) for k_v.

Van der Held (1931) has shown that for values of $\alpha > 1$, the mean fractional absorption for a spectral interval is closely approximated by the Ladenburg-Reiche (1913) formula:

$$A = 1 - \exp[-\beta x e^{-x}(I_o(x) + I_1(x))] \tag{10}$$

where

$$\beta = \frac{2\pi\alpha_L}{d}$$

$$x = \frac{Su}{2\pi\alpha_L}$$

and I_o and I_1 are the Bessel functions of order zero and one and of imaginary argument.

The two equations (9) and (10) give the fractional absorption due to one spectral line. When broad spectral intervals consisting of a large number of lines are considered, the transmission and absorption of a gas can be represented by any one

of several band models. Here we have adopted a "statistical" band model in which the mean line spacing is held constant throughout the band, while the line intensity is allowed to vary from interval to interval within the band. So, if the mean line spacing d for the whole band and mean line intensity S for each one of the spectral intervals within the band are known, the average transmission or absorption in each of the spectral intervals can be calculated from equations (9) and (10).

The 15 μ CO_2 band was divided into six spectral intervals of 50 cm^{-1} width from 550 cm^{-1} to 850 cm^{-1}. The Lorentz half-width α_L of the lines in this band is given as 0.064 cm^{-1} by Kaplan and Eggers (1956) for a temperature of 298° K and a pressure of one atmosphere. Yamamoto and Sasamori (1958) have used a mean line spacing d of 1.55 cm^{-1} in their calculation of the absorption of this band. Thus, a value of the parameter β is determined as 0.24. With this knowledge of the magnitude of β, another parameter, $S/2\pi\alpha_L$, was deduced for the various spectral intervals from the transmission tables of Stull, Wyatt and Plass (1963). This parameter is given in Table IA.

The 9.6 μ O_3 band was treated as a single spectral interval extending from 990 cm^{-1} to 1090 cm^{-1}. Plass (1960) had made an analysis of the 9.6 μ O_3 band area measurements by Walshaw (1957) and so had evaluated the parameters β and $S/2\pi\alpha_L$ for this band. It was found that the values obtained by Plass can reproduce the band area as measured by Walshaw quite accurately

and so they were adopted in our investigation. The Lorentz half-width of the spectral lines in the 9.6 μ O_3 band is given by Goody (1964) as 0.076 cm^{-1} at 293° K and 1000 mb. Using this value, the quantities S and d can be obtained (Table IB).

The value of the Doppler half-width α_D at a temperature of 225° K is also given in these tables for both bands.

Using these values of the various band parameters, the fractional absorption is calculated from equations (9) and (10) for different path lengths and pressures. As an illustration, the absorption obtained for the 15 μ CO_2 and 9.6 μ O_3 bands, plotted as a function of $2\pi\alpha x$, is shown in Figures IV and V. In these figures, lines of constant values of the parameter α are shown. Each of these lines corresponds to a line of constant pressure if the temperature remains unchanged at 225° K. For low pressures (small α) the absorption is mainly due to the Doppler broadening and, with the increase of path length, the absorption increases very slowly until the wings of the absorption lines gradually begin to absorb. Then the absorption increases in square root fashion with path length until the level of saturation is reached.

In calculation of atmospheric transmissions over long path lengths, the variation of pressure and temperature must be taken into account. Therefore, the weighting procedure developed by Curtis (1952) and Godson (1953) was used to obtain the transmission. The temperature dependence of the line strengths

in the 15 μ CO_2 band is treated in a way similar to that used by Praphakara and Hogan (1965). The variation of α with temperature is also incorporated in the calculation.

TABLE I

Band Parameters

A. 15μ CO_2 Band

$\Delta\nu$ (cm^{-1})	a_L (cm^{-1})	d (cm^{-1})	$S/2\pi a_L$ ($atm^{-1}\ cm^{-1}$)	S ($atm^{-1}\ cm^{-2}$)	a_D (cm^{-1})
550-600			1.0×10^{-2}	4.0×10^{-3}	
600-650			2.5×10^{0}	1.0×10^{0}	
650-700	6.4×10^{-2}	1.6×10^{0}	4.5×10^{1}	1.8×10^{1}	6.5×10^{-4}
700-750			5.0×10^{-1}	2.0×10^{-1}	
750-800			2.0×10^{-3}	8.0×10^{-4}	
800-850			2.5×10^{-5}	1.0×10^{-5}	

B. 9.6μ O_3 Band

990-1090	7.6×10^{-2}	6.3×10^{-2}	5.3×10^{-1}	2.5×10^{-1}	9.5×10^{-4}

Results and Discussion

We have examined the infrared radiative heating corresponding to the rocket-measured temperature profiles at Kronogard (66° N, 29 July, 1963) and Barrow (71° N, 9 August, 1965) and determined the vertical velocities in these cases by the procedure outlined above. The heating rates and resultant vertical velocities are given in Figures II and III.

The convergence of infrared flux between 70 km and 90 km altitude leads to a significant diabatic heating of the order of 10° K/day. This heating alone implies vertical velocities of $\sim$ 5 cm/sec near 80 km. This is a consequence of a nearly adiabatic temperature gradient in this region of the atmosphere.

Calculations of infrared heating rates were made for CO_2 vibrational relaxation times λ of 10^{-5} sec and 5×10^{-6} sec (at a pressure of 1 atmosphere) to illustrate the effect of this parameter on the vertical velocities. The vibrational relaxation time of the ν_2 fundamental of CO_2 (15 μ band) is known to within an order of magnitude, 10^{-5} sec to 10^{-6} sec (Marriott, 1964). This relaxation time is inversely proportional to pressure and many have a weak temperature dependence (Herzfeld and Litovitz, 1959). We have considered only the pressure dependence as variations in pressure in the atmosphere are much larger than temperature variations. It can be seen in Figures II and III, that decreasing the relaxation time increases the infrared heating. Were the atmosphere in a state of local thermodynamic

equilibrium at these levels, heating rates in excess of 20° K/day and vertical velocities in excess of 10 cm/sec would be obtained.

Infrared transfer of energy in the 6.3 μ and far infrared rotation bands of H_2O was not taken into account in this study. Estimates of the water vapor content in the high atmosphere differ markedly (see Theon, Nordberg and Smith, 1966). We believe that the presence of significant amounts of water vapor would only augment the infrared flux convergence in the cold region of the atmosphere around 85 km, and result in larger vertical velocities.

Solar ultraviolet heating by O_3 has not been considered here, as the interaction of O_3 with H_2O at these levels would reduce the concentration of O_3 and its heating effect quite drastically (Hunt, 1966; Hessvedt, 1965). Since the amount of H_2O present near the mesopause is uncertain, elaborate photochemical calculations to determine the O_3 concentration were not made. Any ozone heating in the vicinity of the mesopause would contribute to increase the vertical velocities.

In view of the uncertainties of the heating by H_2O in the infrared and by O_3 in the ultraviolet, a detailed determination of the meridional circulation involving horizontal heat transport has not been made here. The cold air advection which one might expect at higher levels in the summer mesosphere would tend to compensate in part for the strong infrared flux convergence at these levels. However, we feel that these estimates of vertical

velocities of ~ 5 cm/sec near 80 km, although somewhat larger than those of Murgatroyd and Singleton (1961), ~ 1 cm/sec, are quite reasonable in view of the extremely cold temperatures observed at these levels.

The vertical velocities derived here might be related to the occurrence of noctilucent clouds in the vicinity of the earth's mesopause. An extensive review of noctilucent cloud studies is given by Fogle and Haurwitz (1966). Noctilucent cloud displays are observed to be quite widespread and thus imply the existence of large scale vertical motions. Charleson (1965) concludes that vertical velocities of the order of 20 cm/sec are required to sustain a cloud of spherically shaped particles of 0.1 μ size with a mean density of ~ 1.0 g/cc. On the other hand, Chapman and Kendall (1965) estimate that, if the particles are of needle or flaky form with a mean density of ~ 0.1 g/cc, vertical velocities of ~ 1 cm/sec (as suggested by Murgatroyd and Singleton (1961)) would be sufficient for cloud formation. The vertical velocities of ~ 5 cm/sec which are suggested by this study, when extremely cold temperatures are present, would favor theories of noctilucent cloud formation based upon less restrictive assumptions with regard to particle shape, size and density.

Acknowledgements

Our thanks to Mr. Ludwig Umscheid of Computer Applications, Inc. for his expert programming of the problem.

This research was supported in part by National Aeronautics and Space Administration Grant Number Ns G - 499 to New York University.

REFERENCES

Chapman, S., and P. C. Kendall, 1965: Noctilucent clouds and thermospheric dust: their diffusion and height distribution. Quart. J. Roy. Met. Soc., 91, 115 - 131.

Charleson, R. J., 1965: Noctilucent clouds: a steady-state model. Quart. J. Roy. Met. Soc., 91, 517 - 523.

Curtis, A. R., 1952: Discussion of Goody's "A statistical model for water vapor absorption. Quart. J. Roy. Met. Soc., 78, 638 - 640.

Curtis, A. R., and R. M. Goody, 1956: Thermal radiation in the upper atmosphere. Proc. Roy. Soc., 236A, 193 - 206.

Fogle, B., and B. Haurwitz, 1966: Noctilucent clouds. Space Sci. Rev., VI, 278 - 340.

Godson, W. L., 1953: The evaluation of infrared radiative fluxes due to atmospheric water vapor. Quart. J. Roy. Met. Soc., 79, 376 - 379.

Goody, R. M., 1964: Atmospheric radiation, Vol. 1. Clarendon Press, Oxford, 435 pp.

Harris, D. L., 1948: On the line-absorption coefficient due to the Doppler effect and damping. Ap. J., 108, 112 - 115.

Herzfeld, K. F., and T. A. Litovitz, 1959: Absorption and dispersion of ultrasonic waves. Academic Press, New York, 535 pp.

Hessvedt, E., 1965: Some characteristics of the oxygen - hydrogen atmosphere. Geofysiske Publikasjoner Geophysica Norvegica, XXVI, 1 - 30.

Hines, C., 1963: The upper atmosphere in motion. Quart. J. Roy. Met. Soc., 89, 1 - 42.

Hunt, B. G., 1966: Photochemistry of ozone in a moist atmosphere. J. Geophys. Res., 71, 1385 - 1397.

Kaplan, L. D., and D. F. Eggers, 1956: Intensity and linewidth of the 15μ CO_2 band, determined by a curve of growth method. J. Chem. Phys., 25, 876 - 883.

Kellogg, W. W., 1961: Chemical heating above the polar mesopause in winter. J. Meteor., 18, 373 - 381.

Ladenburg, R., and F. Reiche, 1913: Über selektive Absorption. Ann. d. Phys., 42, 181.

Leovy, C., 1964: Simple models of thermally driven mesospheric circulation. J. Atmos. Sci., 21, 327 - 341.

_____, 1966: Photochemical destabilization of gravity waves near the mesopause. J. Atmos. Sci., 23, 223 - 232.

Marriott, R., 1964: Molecular collision cross sections and vibrational relaxation in carbon dioxide. Proc. Phys. Soc., 84, 877 - 888.

Murgatroyd, R. J., and R. M. Goody, 1958: Sources and sinks of radiative energy from 30 to 90 km. Quart. J. Roy. Met. Soc., 84, 224 - 234.

Murgatroyd, R. J., and F. Singleton, 1961: Possible meridional circulations in the stratosphere and mesosphere. Quart. J. Roy. Met. Soc., 87, 125 - 135.

Plass, G. N., 1960: Useful representations for measurements of spectral band absorption. J. Opt. Soc. Amer., 50, 868 - 875.

Prabhakara, C., and J. S. Hogan, 1965: Ozone and carbon dioxide heating in the Martian atmosphere. J. Atmos. Sci., 22, 97 - 109.

Stull, V. R., P. J. Wyatt and G. N. Plass, 1963: The infrared absorption of carbon dioxide. Infrared transmission studies III, Rept. Contract SSD-TDR-62-127, Space Systems Division, Air Force Systems Command, Los Angeles, California.

Theon, J. S., W. Nordberg, and W. S. Smith, 1966: Measured temperature structure in noctilucent clouds. X-621-66-597, Goddard Space Flight Center, Greenbelt, Md.

van der Held, E. F. M., 1931: Intensitat und natürliche Breite von Spektrallinien. Z. Phys., 70, 508 - 515.

Walshaw, C. D., 1957: Integrated absorption by the 9.6μ band of ozone. Quart. J. Roy. Met. Soc., 83, 315 - 321.

Yamamoto, G., and T. Sasamori, 1958: Calculations of the absorption of the 15μ carbon dioxide band. Science Reports, Tohoku University, 5th Series (Geophysics), 10, 37 - 57.

FIGURE CAPTIONS

Figure I: Typical high latitude summertime and wintertime temperature profiles. These averages include soundings from Churchill, Barrow and Kronogard. (After Theon, Nordberg and Smith, 1966.)

Figure II: Observed summer temperatures (heavy solid line), calculated infrared heating rates and resultant vertical velocities ((A) light solid lines, $\lambda_o = 10^{-5}$ sec; (B) dashed lines, $\lambda_o = 5 \times 10^{-6}$ sec) at Kronogard, Sweden.

Figure III: Observed summer temperatures (heavy solid line), calculated infrared heating rates and resultant vertical velocities ((A) light solid lines, $\lambda_o = 10^{-5}$ sec; (B) dashed lines, $\lambda_o = 5 \times 10^{-6}$ sec) at Barrow, Alaska.

Figure IV: Absorption by mixed Doppler and Lorentz lines in the 15μ CO_2 band. The abscissa $2\pi\alpha x = Su/\alpha_D$, and $d/\alpha_D = 2.46 \times 10^3$.

Figure V: Absorbtion by mixed Doppler and Lorentz lines in the 9.6μ O_3 band. The abscissa $2\pi\alpha x = Su/\alpha_D$, and $d/\alpha_D = 66.3$.

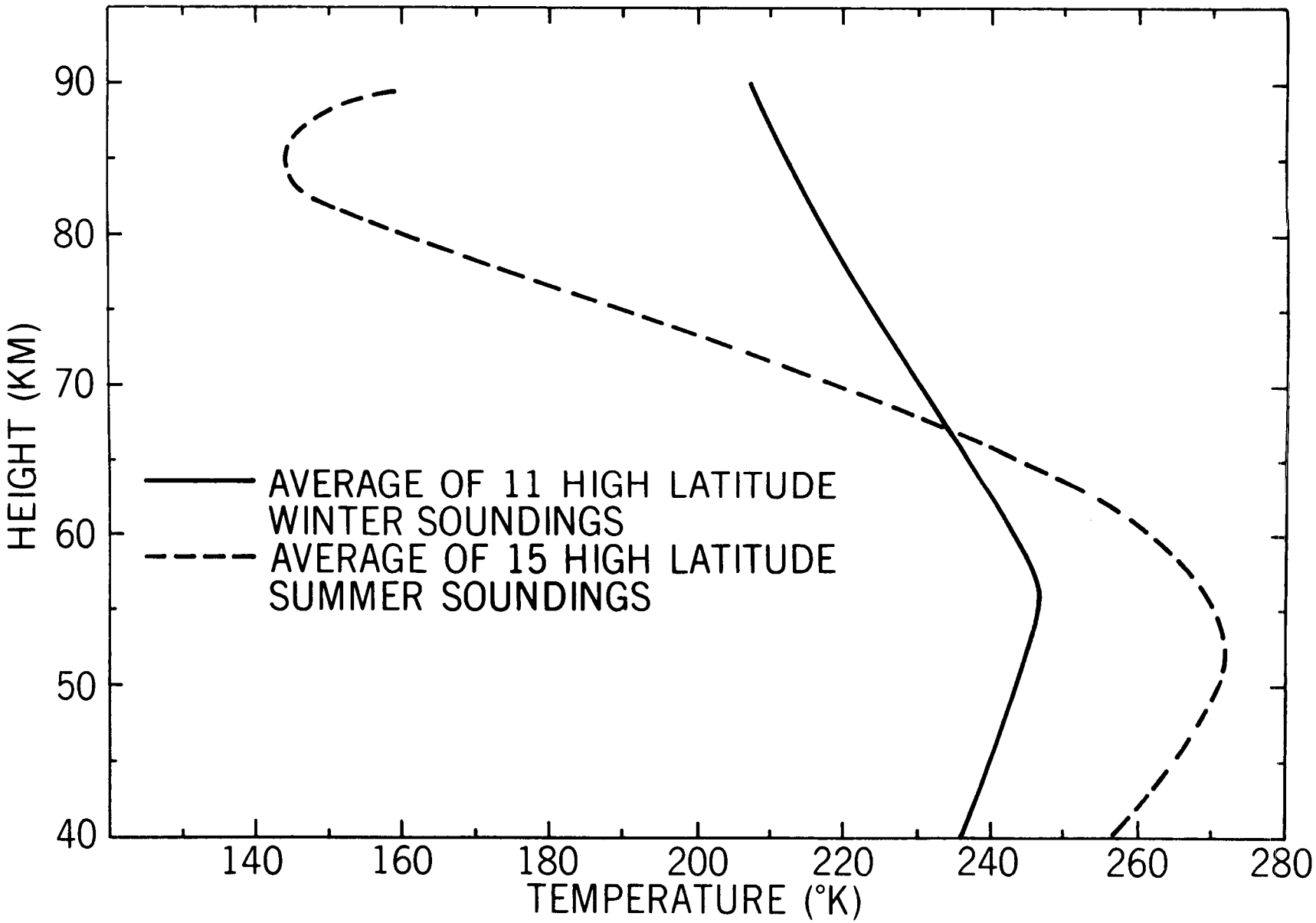
90
80
70
60
50
40
HEIGHT (KM)
AVERAGE OF 11 HIGH LATITUDE WINTER SOUNDINGS
AVERAGE OF 15 HIGH LATITUDE SUMMER SOUNDINGS
140
160
180
200
220
240
260
280
TEMPERATURE (°K)

Figure I

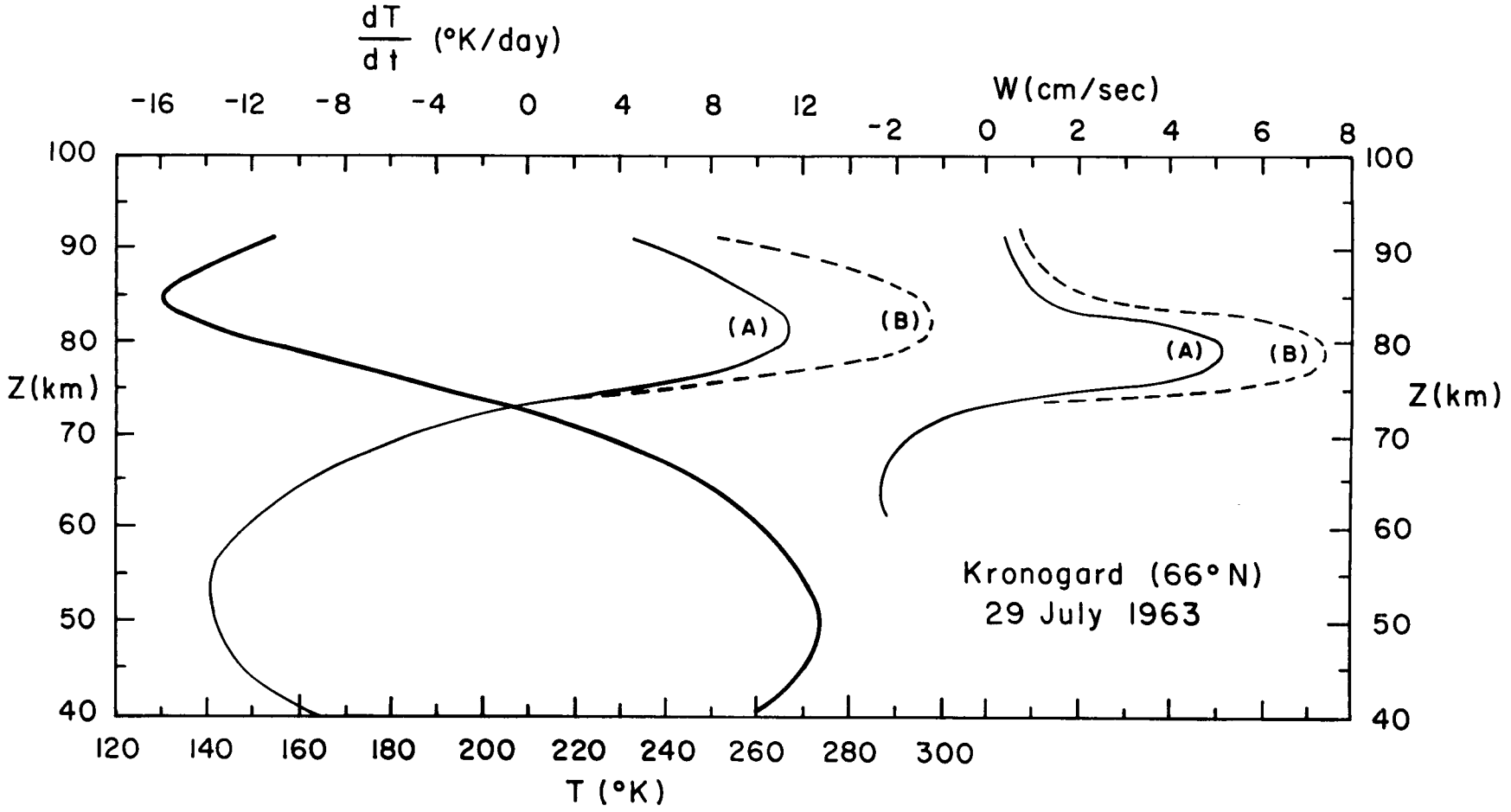
dT/dt (°K/day)
-16 -12 -8 -4 0 4 8 12
W(cm/sec)
-2 0 2 4 6 8
100 90 80 70 60 50 40
Z(km)
(A)
(B)
(A)
(B)
Kronogard (66° N)
29 July 1963
120 140 160 180 200 220 240 260 280 300
T (°K)

Figure II

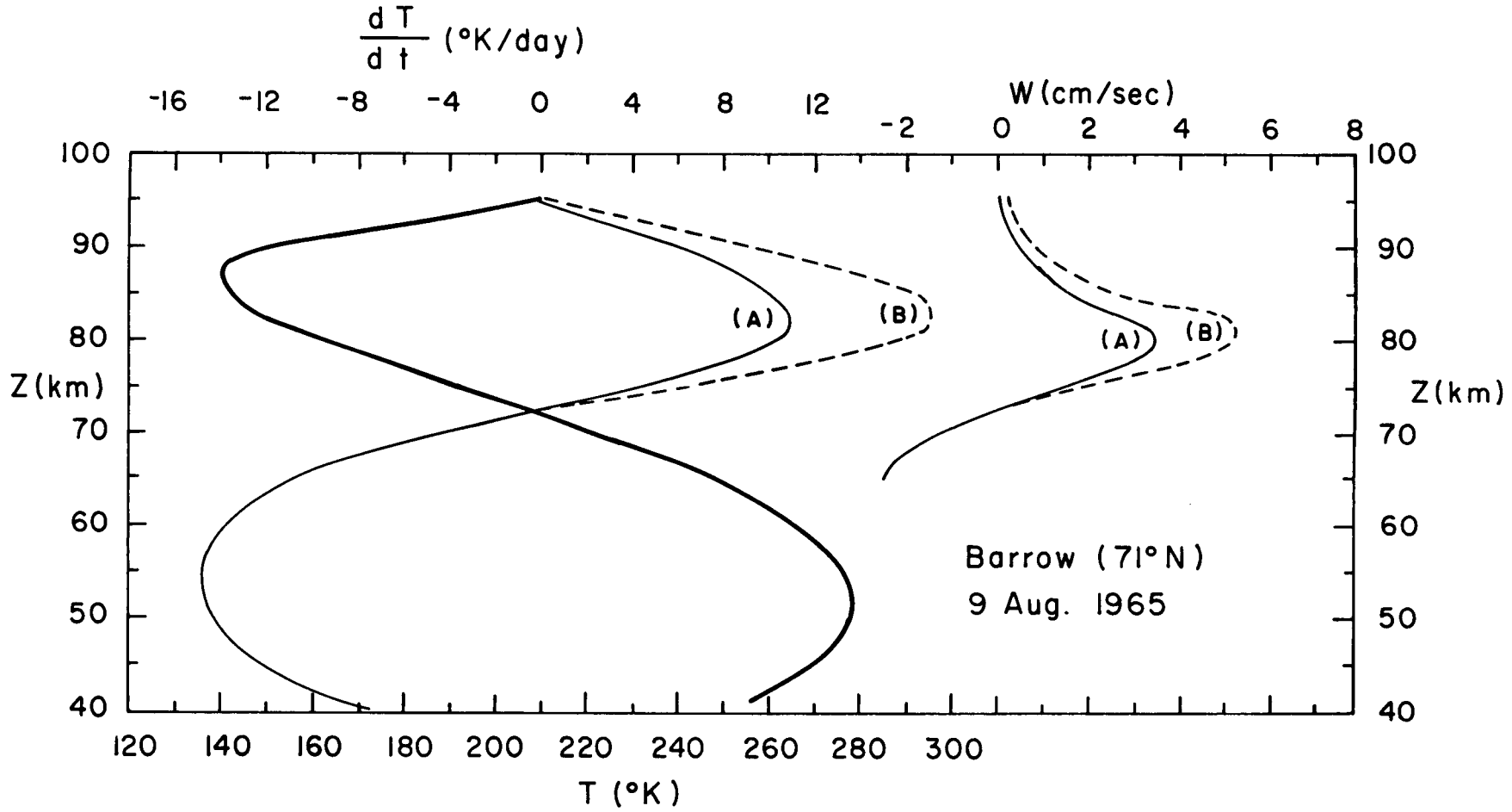
dT/dt (°K/day)
-16 -12 -8 -4 0 4 8 12
W (cm/sec)
-2 0 2 4 6 8
100
90
80
70
60
50
40
Z(km)
(A)
(B)
(A)
(B)
Barrow (71° N)
9 Aug. 1965
120 140 160 180 200 220 240 260 280 300
T (°K)

Figure III

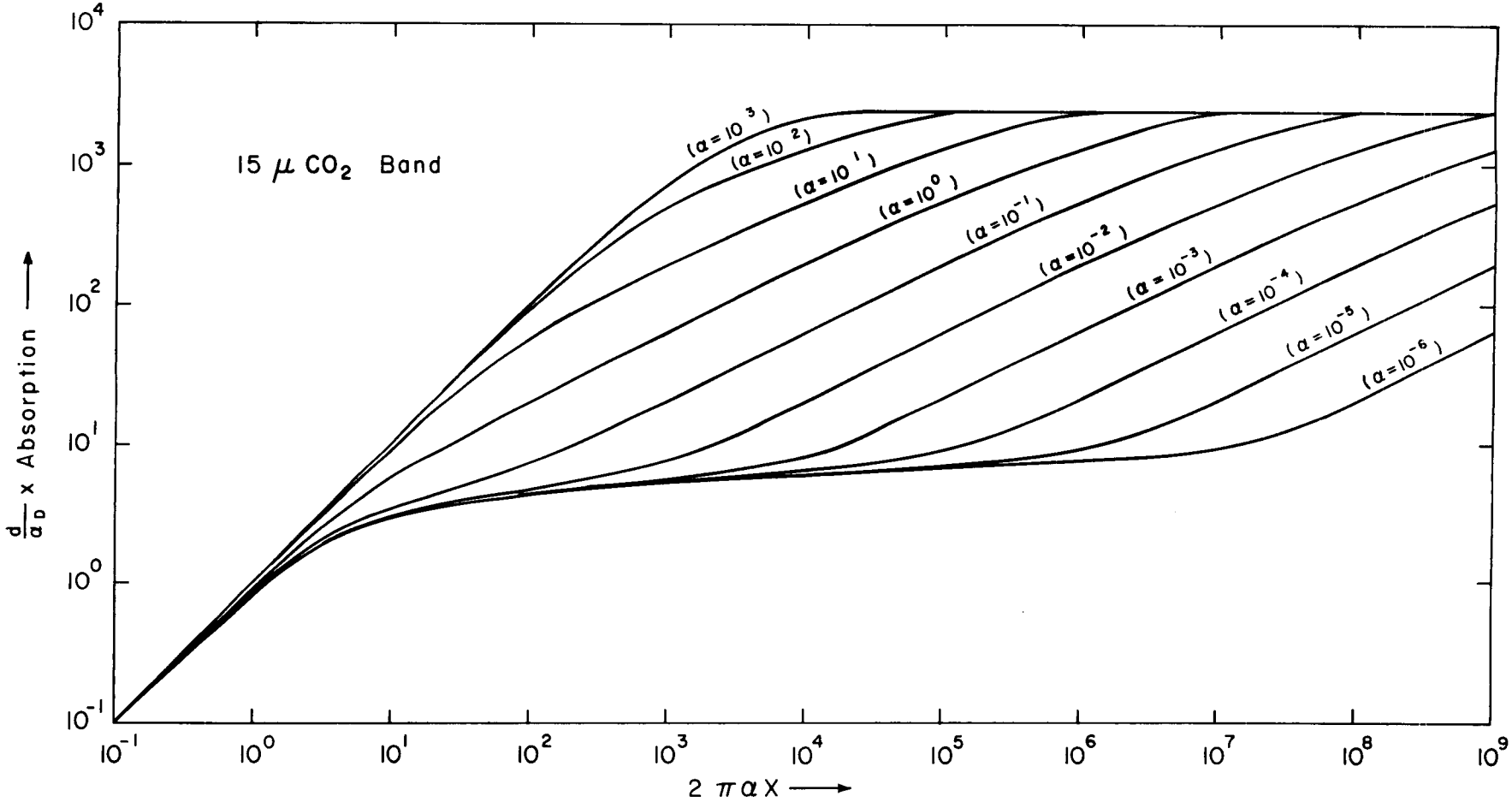
15 μ CO2 Band
(α=10^3)
(α=10^2)
(α=10^1)
(α=10^0)
(α=10^-1)
(α=10^-2)
(α=10^-3)
(α=10^-4)
(α=10^-5)
(α=10^-6)
d/αD x Absorption
2 π α X
10^4
10^3
10^2
10^1
10^0
10^-1
10^-1
10^0
10^1
10^2
10^3
10^4
10^5
10^6
10^7
10^8
10^9

Figure IV

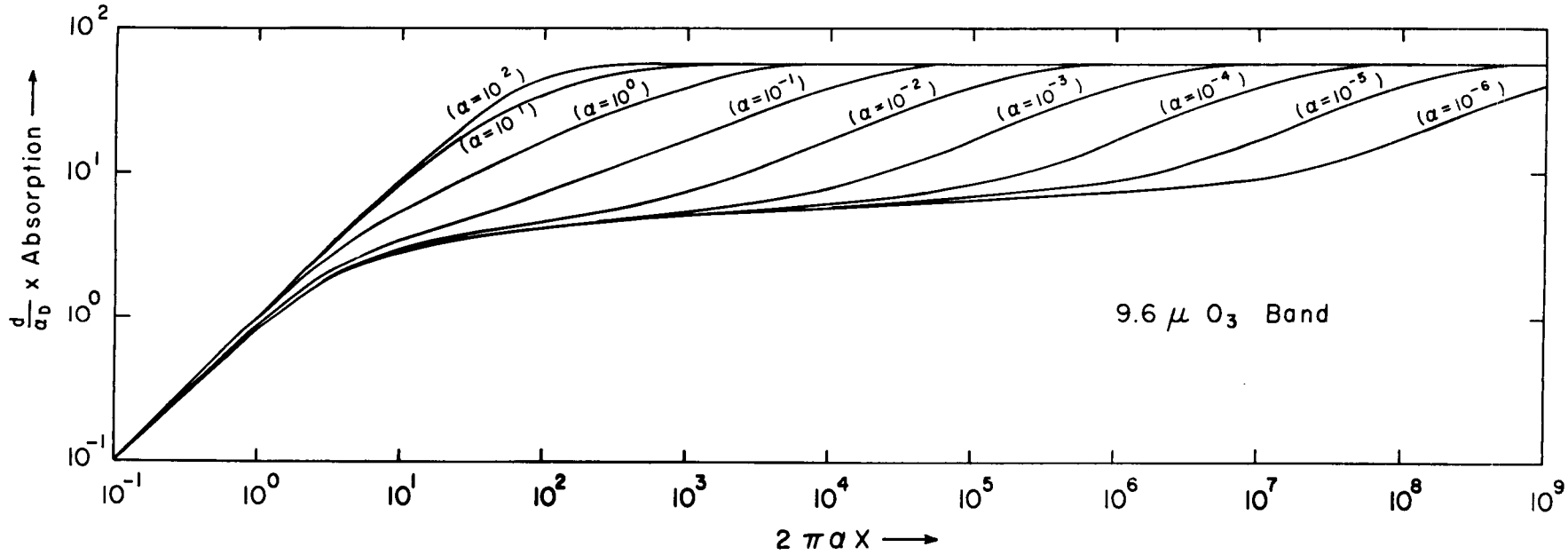
10^2
10^1
10^0
10^{-1}
$\frac{d}{a_0}$ x Absorption ⟶
$(a=10^2)$
$(a=10^1)$
$(a=10^0)$
$(a=10^{-1})$
$(a=10^{-2})$
$(a=10^{-3})$
$(a=10^{-4})$
$(a=10^{-5})$
$(a=10^{-6})$
9.6 μ O_3 Band
10^{-1} 10^0 10^1 10^2 10^3 10^4 10^5 10^6 10^7 10^8 10^9
$2\pi a x$ ⟶

Figure V